ACS APPLIED NANO MATERIALS

Article

Predicting Nanoparticle Suspension Viscoelasticity for Multimaterial 3D Printing of Silica-Titania Glass

Nikola A. Dudukovic, Lana L. Wong, Du T. Nguyen, Joel F. Destino, Timothy D. Yee, Frederick J. Ryerson, Tayyab Suratwala, Eric B. Duoss, and Rebecca Dylla-Spears

ACS Appl. Nano Mater., **Just Accepted Manuscript** • DOI: 10.1021/acsanm.8b00821 • Publication Date (Web): 17 Jul 2018

ACS Publications

is published by the American Chemical Society. 1155 Sixteenth Street N.W., Washington, DC 20036

Predicting Nanoparticle Suspension Viscoelasticity for Multimaterial 3D Printing of Silica-Titania Glass

Nikola A. Dudukovic[1*], Lana L. Wong[1], Du T. Nguyen[1], Joel F. Destino[1,2], Timothy D. Yee[1], Frederick J. Ryerson[1], Tayyab Suratwala[1], Eric B. Duoss[1], Rebecca Dylla-Spears[1]

[1]Lawrence Livermore National Laboratory, Livermore, CA 94551, USA
[2]Department of Chemistry, Creighton University, Omaha, NE 68178, USA

ABSTRACT: A lack of predictive methodology is frequently a major bottleneck in materials development for additive manufacturing. Hence, exploration of new printable materials often relies on the serendipity of trial and error approaches, which is time-consuming, labor-intensive, and costly. We present an approach to overcome these issues by quantifying and controlling the viscoelasticity of inks for multimaterial 3D printing of silica-titania glass using direct ink writing (DIW). We formulate simple silica and silica-titania inks from a suspension of fumed silica nanoparticles in an organic solvent with a dissolved molecular titania precursor. We use a small set of experimental rheological data and estimates of interaction potentials from colloidal theory to develop a predictive tool that allows us to design and obtain compatible inks that are matched both in desired rheological properties (viscosity profiles and elastic modulus) as well as solids loading. The model incorporates silica particle volume fraction, particle size, particle size distribution, and titania precursor concentration, and captures the effects of all formulation parameters on the measured viscoelasticity in a single curve. We validate the ink formulations predicted by the model and find that the materials can be very well matched in rheological properties as desired for 3D printing. Using DIW and heat treatment methods we have reported previously, we use these inks to print and process a fully transparent glass with spatial change in dopant composition and refractive index. We believe that this approach can be extended to other colloidal systems and allow predictive ink formulation design for desired printability in direct ink write manufacturing.

KEYWORDS: *3D printing, direct ink writing, multimaterial, glass, colloids, rheology*

* Corresponding author: Nikola Dudukovic, dudukovic1@llnl.gov

INTRODUCTION

Additive manufacturing (AM) continues to open new routes to production of high performance structures with properties that are unattainable by conventional fabrication methods. The rapid growth of the 3D printing industry has driven research efforts to expand the existing palette of printable materials.[1] In particular, silica glass is a highly desirable material for numerous applications, due to its transparency, chemical and thermal resistance, and mechanical properties. These characteristics can be enhanced by addition of dopants, as in the case of silica-titania (SiO_2-TiO_2) glasses, which can impart modifications in the optical (e.g. change in refractive index) or mechanical (e.g. ultralow thermal expansion) properties of the material.[2] The ability to 3D print transparent glass could enable advanced applications ranging from microfluidics to optics. Moreover, multimaterial printing gives rise to a diverse set of functionalities by providing spatial control of material composition in the printed construct. In this regard, multimaterial 3D printing of ceramics and glasses can expand the design space for advanced freeform optics with tailored properties, such as waveguides, mirrors, gradient index (GRIN) lenses, and

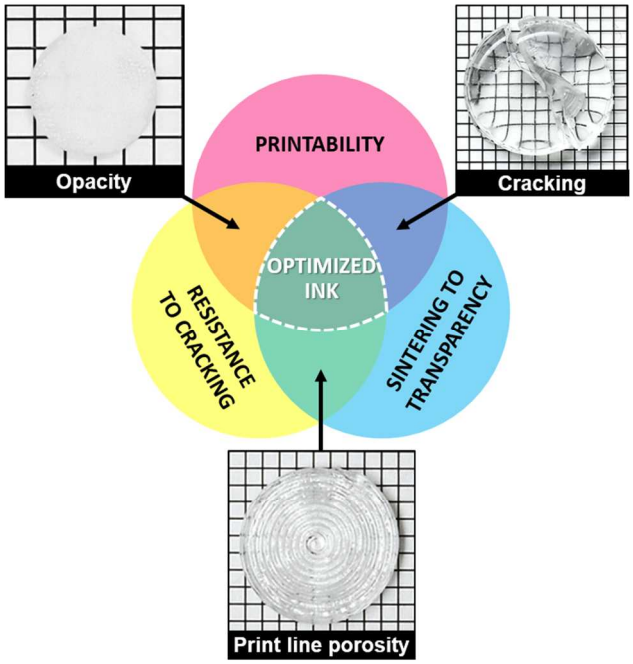

Figure 1. Ink formulation requirements. The post-print treatment is sensitive to chemical modification of the ink, which can result in unwanted subsequent porosity (i.e. lack of transparency) or decreased green body strength (i.e. cracking).

laser rods.[3]

Several methods for glass AM have been reported,[4, 5] including direct selective laser sintering and melting (printing by thermal or laser melting of glass filaments or powders)[6-8] and microstereolithography (layer-by-layer photopatterning of a silica-loaded photopolymer resin).[9] Recently, our group demonstrated a direct ink writing (DIW) approach to printing silica and silica-titania glass from fumed silica suspensions[10] and sol-gel feedstocks.[11] In DIW, a viscoelastic shear-thinning

material ("ink") is extruded through a nozzle in a programmed pattern. Upon exiting the nozzle, the extruded material rapidly re-solidifies via gelation, evaporation, chemical reaction, or temperature-induced phase change to form a filamentary shape.[12] Using this method, a three-dimensional object is built up layer-by-layer. In our approach, we print a glass preform from a silica-loaded ink. The printed object is then thermally treated to dry the printed part, remove any organic components, and sinter to form a dense, transparent glass.

The central challenge in glass DIW is optimizing the ink formulation for a complex combination of factors. In addition to formulating an ink that is printable, i.e. possesses the desired rheological characteristics (storage and loss modulus, shear viscosity, elastic recovery, etc.), the printed structure also needs to withstand the subsequent thermal treatment without cracking, and achieve full transparency at the end of the sintering process **(Figure 1)**. These requirements impose stringent limits on the tolerance for chemical modification of the inks. For multimaterial glass printing, these constraints become even more rigorous – the inks need to not only have matching flow properties, but also contain the same solids loading. Discrepancies in the solids concentration in the printed object produce differential shrinkage stresses that lead to cracking during the thermal treatment. Conversely, discrepancies in the rheological properties result in dissimilar flow behavior during extrusion, making printing multiple materials together increasingly difficult. Moreover, even for single-material printing, adjustment of the printing setup (e.g. nozzle diameter and height) and re-adjustment of printing parameters (flow rate, print speed, nozzle height, etc.) are required whenever a meaningful change in ink formulation (or a new material altogether) is introduced. This process is complicated and time-consuming, and thus significantly hinders the usefulness and versatility of DIW for any cost-effective manufacturing setup. Therefore, the ability to predict and tailor the viscoelastic properties of the ink for a given set of printing parameters is imperative. While some investigations have focused on optimizing the extrusion process for a given material,[13, 14] here we attempt to instead tune the behavior of multiple materials to exhibit the same printability for a fixed set of printing parameters.

To achieve this, we have developed an approach to quantify and regulate ink viscoelasticity for multimaterial 3D printing of silica and silica-titania glass using direct ink writing (DIW). We devise a predictive model that captures the effects of silica particle volume fraction, particle size, particle size distribution, and surfactant (molecular TiO_2 precursor) concentration in a single expression. This approach allows us to design and produce inks with matching desired rheological properties at the same total solids loading, while minimizing chemical alterations.

▪ EXPERIMENTAL SECTION

Materials. Hydrophilic fumed silica nanoparticles in dry powder form (CAB-O-SIL® EH5, Cabot Corporation; AEROSIL® OX50 and AEROSIL® TT600, Evonik Industries) were used in all inks. The average nominal particle sizes were estimated from TEM images (Figure S1) and used as the effective particle sizes in subsequent calculations. Tetraethylene glycol dimethyl ether (tetraglyme) ≥99% and titanium

diisopropoxide bis(acetylacetonate) (75 wt.% in isopropanol) were obtained from Sigma-Aldrich and used as received. The ink components are summarized in **Table 1**.

Ink preparation. The silica-only suspensions were prepared by adding one or two types of hydrophilic fumed silica particles at desired ratios and tetraglyme to a container, followed by mixing in a THINKY planetary mixer at 2000 rpm for 2 min. To create inks for printing titania-doped silica glass, a molecular titania precursor (titanium diisopropoxide bis(acetylacetonate)) was added to the mixture. The precursor (referred to as TBDA from here on), which is converted to TiO_2 at elevated temperatures (> 500 °C), was used in amounts required to obtain 2, 4, 6, 8, or 10 wt% of TiO_2 in the final glass. The mass of TBDA needed to achieve the desired TiO_2 doping in the glass was calculated as:

$$m_{TBDA} = m_{SiO2} \frac{x_{TiO2}}{1 - x_{TiO2}} \frac{MW_{TBDA}}{MW_{TiO2}} \quad (1)$$

where x_{TiO2} is the mass fraction of TiO_2 in the final glass, m_i is the measured mass and molecular weight of the ink component, and MW_i are the molecular weights of TBDA and TiO_2 (364.26 g/mol and 79.866 g/mol, respectively. The volume fraction of TBDA was estimated as:

$$\phi_{TBDA} = \frac{m_{TBDA}}{\rho_{TBDA} V_{tot}} \quad (2)$$

where ρ_{TBDA} = 1.092 g/mL is the density of TBDA and V_{tot} is the total ink volume. A conversion table between the desired TiO_2 concentrations in the final glass product and the required volume fractions of TBDA used in this work, as well as the full ink compositions for all samples, are available in the Supporting Information (Tables S1 and S2).

Table 1. Ink compositions for printing silica and silica-titania glass.

Ink	Particles	Nominal size	Solvent	Dopant
Silica	CAB-O-SIL EH5	22 nm	Tetraglyme (tetraethylene glycol dimethyl ether) 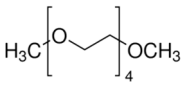	
	AEROSIL OX50	50 nm		
	AEROSIL TT600	75 nm		
Silica-titania	CAB-O-SIL EH5	22 nm		TBDA (titanium diisopropoxide bis(acetylacetonate)) 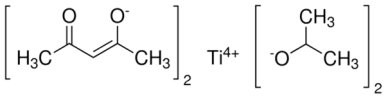

Rheology measurements. Viscosity and shear moduli measurements were performed on a TA Instruments DHR-1 rotational rheometer, using a 25-mm stainless steel parallel plate setup. The temperature of the Peltier plate was kept at 23 °C (to match the ambient conditions of the 3D printing process) via active water circulation from an external pump through the cooling jacket of the Peltier cell. The sample thickness (spacing between the plates) was set to 500 µm. Ink viscosities were measured at shear rates ranging from 0.01 to 100 s^{-1}. Thixotropic hysteresis measurements were done by

consecutively ramping the shear rate up and down in the described range, performing multiple cycles. Oscillatory shear measurements of the elastic and viscous moduli were performed at a constant frequency of 1 Hz. The average of the shear modulus in the linear viscoelastic region was used in all subsequent calculations.

Zeta potential measurements. Samples were analyzed for zeta potential by Micromeritics Analytical Services (Norcross, GA) using electrophoretic light scattering (Particulate Systems NanoPlus HD-3). The measurements were performed at dilute fumed silica particle concentrations of 0.5-2 wt% in tetraglyme, for SiO_2/tetraglyme-only and SiO_2/TBDA/tetraglyme mixtures.

Transmission electron microscopy (TEM). As-received fumed silica samples were diluted to ~0.01 wt% solids in ethanol (Pharmco-AAPER, 200 Proof ACS/USP Grade, ≥ 99.5%) and sonicated for several minutes. Samples for microscopy were prepared by drop casting 5 µL of the ethanolic silica solution onto an ultrathin carbon film on lacy carbon support film Cu mesh (Ted Pella) and allowed to dry under ambient conditions. Electron micrographs were acquired with an FEI Titan transmission electron microscope (TEM) operating at an accelerating voltage of 300 kV.

Glass composition characterization. The compositional microanalyses were collected on a JEOL-8200 electron microprobe operating at 15 kV with a beam current of 25 nA. The beam diameter was 5 µm and the analysis positions were spaced 10 µm apart. X-ray intensities were measured for the $Ti_{k\alpha}$ and $Si_{k\alpha}$ lines with peak count times of 30 s. $Ti_{k\alpha}$ was analyzed by combining the intensities from 3 wavelength spectrometers equipped with PET crystals, yielding errors from counting statistics less than 1% relative. Background intensities were determined using a mean atomic number (MAN) background calibration curve method as described by Donovan *et al.*[15] and X-ray intensities were converted to oxide compositions using the CITZAF correction scheme[16] with TiO_2 and SiO_2 as primary standards for Ti and Si, respectively.

Direct ink writing.

The 3D printing process was accomplished on a DIW setup with a three-axis micropositioning bottom stage. The inks were loaded into 30 mL syringes, affixed above the build plate, and connected via Teflon tubing to a Y-shaped double-inlet, single-outlet nozzle of a 610 µm diameter. Constant displacement drives were used to deliver the inks by moving the pistons at rates required to provide a linear printing speed of 10 mm/s. The glass preforms (20 mm diameter, 5 mm height cylinders) were printed in 12 layers using an Archimedes spiral pattern. The displacement pistons were programmed to switch from one material to another within each layer at the 5 mm radius to produce a TBDA-doped core and SiO_2-only cladding. No compensation was used to rectify the inherent capacitance of the system, i.e. the start/stop behavior of the material was not immediate, leading to a smoother profile than the intended sharp step function. To facilitate the visual difference between the two materials, the TBDA-containing ink was doped with a few ppm of Sudan Red dye. A video of the printing process can be found in the Supporting Information.

▪ RESULTS AND DISCUSSION

Desired rheology and effect of TiO_2 precursor. We have previously reported an optimized ink formulation based on CAB-O-SIL® EH5 fumed silica particles dispersed in tetraglyme at 20 wt% (particle volume fraction of $\phi = 0.103$).[10] Tetraglyme was chosen for its high boiling point, which allows finer control over the drying rate during the heat treatment of the printed part. This ink is a gel at room temperature (elastic shear modulus $G' \approx 10^5$ Pa), and a shear-thinning yield stress material, characterized by its absence of a viscosity plateau at low shear rates (**Figure 2a**, purple squares). The rapid elastic recovery of the material upon extrusion provides good filament shape retention.[10] It is worth noting that the viscoelastic behavior of the material during deposition is vital in obtaining a final monolith with no porosity, which is highly specific context of desired printability. This window of viscoelasticity required for desired filament "fusing" is fairly narrow – if the material is too elastic, the entrapment of voids between extruded filaments will result in print-line porosity in the final glass (**Figure 1**). While high elasticity is a very desirable characteristic for printing complex structures and spanning overhangs,[12] it does not provide the right space-filling printability conditions for producing void-free monoliths. On the other hand, if the ink behavior is predominantly viscous, the extruded material will slump, thereby preventing the creation of the anticipated 3D object. We have found that the SiO_2/tetraglyme ink with $\phi = 0.103$ performs optimally in this regard, allowing for a void-free, slump-free monolith to be printed. The relatively high shear modulus and viscosity of this gel at a fairly low volume fraction stem from the formation of a strongly flocculated silica network, which is dominated by interparticle hydrogen bonding in ether-like solvents such as tetraglyme.[17, 18] Consequently, these strong attractions facilitate the crack-free densification of the silica green body during the drying process. Due to these favorable properties, we have adopted the rheological characteristics of this ink as the desired baseline for all further ink development.

To obtain a titania-doped silica glass, we add to our previous formulation TBDA – a molecular precursor to titania, which converts to TiO_2 at elevated temperatures (> 500 °C). Our main interest lies in the 5-8 wt% range of TiO_2 in the final glass, where refractive index changes of 0.02-0.025 and ultralow expansion properties of the glass can be achieved.[2] Using TBDA to attain the doping helps to avoid titania crystallization issues that are often encountered when using TiO_2 nanoparticles, which can result in haziness of the final glass.[2, 19-22] However, incorporating TBDA into the ink, while keeping the total SiO_2 concentration constant, drastically alters the ink rheology, changing the flow curve profile (**Figure 2a**) and lowering the shear modulus and viscosity by several orders of magnitude (**Figure 2b**). Consecutive ramps of increasing and decreasing shear rate show significant hysteresis in TBDA-containing inks (**Figure 2c**). The observed behavior indicates that TBDA acts as a surfactant by forming a solvation layer around the particles, thereby reducing attractions and weakening the particle network. With increasing TBDA concentration, at the same total silica concentration, the inks rapidly lose their shape retention ability, resulting in unfavorable slumping and spreading of the ink upon extrusion. An example of this can be seen in the inset in **Figure 2b**, where increase in TBDA concentration (equivalent to 2, 4, 6, 8, and 10 wt% TiO_2 in the final glass), which also results in a color change, leads to extruded piles that exhibit less structure.

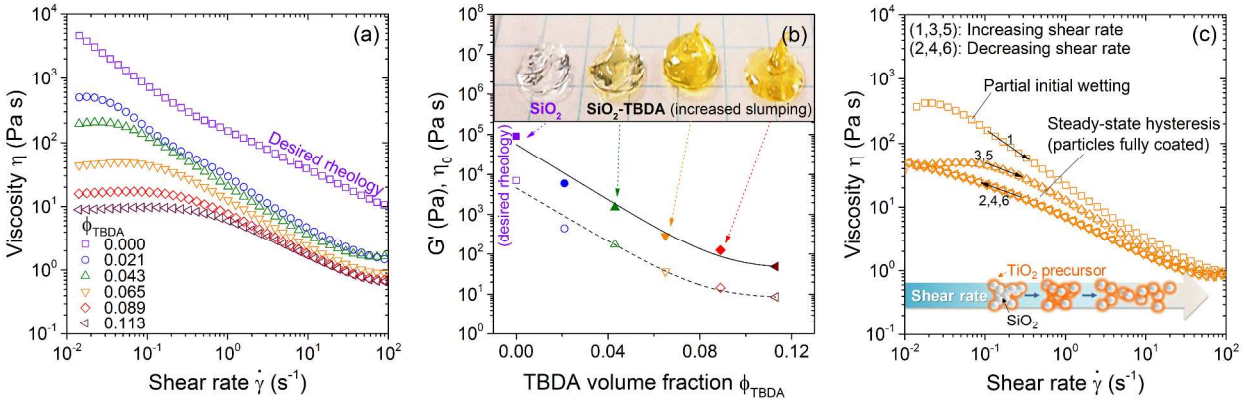

Figure 2. Effect of TiO_2 precursor (TBDA) concentration on ink rheology at constant SiO_2 volume fraction of ϕ = 0.103. (a) While the SiO_2-only ink is a yield stress fluid (gel) with no low-shear plateau, addition of TBDA changes the flow curve profile and exhibits a pronounced zero-shear viscosity, indicating the tendency of the TBDA inks to flow at rest. **(b)** The linear elastic modulus and low-shear viscosity show the same trend and decrease by three orders of magnitude over the TBDA range. **(c)** With increasing shear rate, flocs of silica particles are broken down and particles are uniformly coated with TBDA. Additional data available in Figures S2-S4.

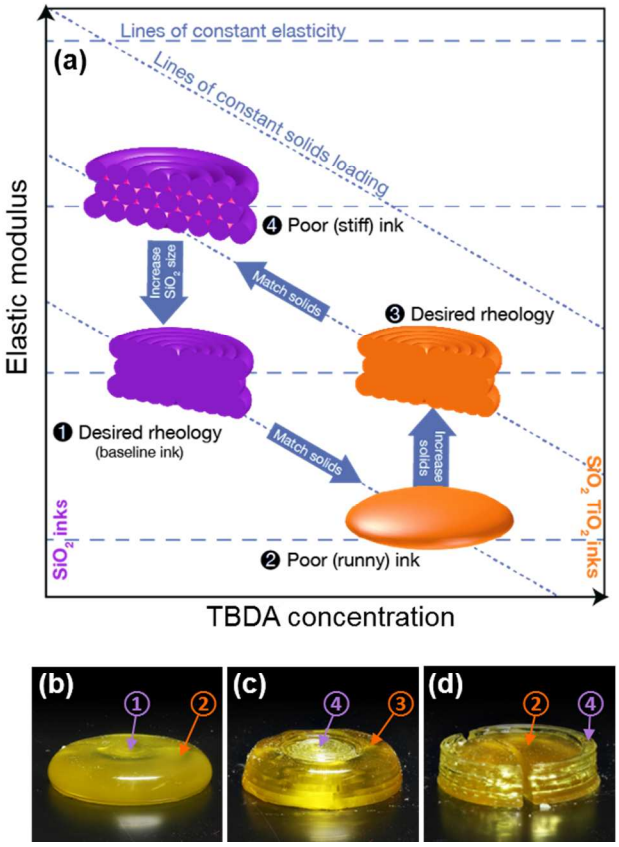

Figure 3. The need for simultaneous matching of the desired rheology and total solids concentration of two inks. (a) To avoid additional chemical species in the material, control over ink properties can instead be achieved by modifying the silica particle volume fraction and particle size/distribution. **(b), (c)** When printing two inks of the same solids concentration but disparate rheological properties, the inks exhibit different printability. **(d)** When inks are mismatched in both rheology and solids concentration, in addition to incompatible printability, cracking due to differential shrinkage stresses occurs even during room temperature air drying.

Matching rheology and solids loading. To alleviate the issues caused by the TBDA without using additional chemical agents, one could simply increase the particle volume fraction in the TBDA-containing ink to increase the viscosity and modulus to the desired value. However, for *multimaterial printing* (SiO_2 and SiO_2-TBDA inks), this would result in a mismatch of solids loading between the two inks, thereby introducing differential shrinkage stresses during the drying stage, which leads to cracking. On the other hand, increasing the solids loading in both inks would lead to unfavorable stiffening of the SiO_2-only ink.[10] For particles of different sizes but same surface chemistry, the elastic modulus is expected to scale with particle size as $G' \sim a^{-3}$.[23] Hence, our solution is to control the particle size and size distribution in addition to particle volume fraction, as opposed to introducing chemical modifiers such as surfactants or salts that could affect the final glass properties **(Figure 3)**. Four sets of data using EH5 (22 nm) and OX50 (50 nm) fumed silica were collected to examine the isolated effects of particle volume fraction, particle size, particle size distribution, and surfactant (TBDA) concentration. The data illustrates that the elastic modulus decreases with: (1) decreasing SiO_2 volume fraction, (2) increasing OX50:EH5 particle ratio in bimodal silica mixtures, and (3) increasing TBDA concentration **(Figure 4a)**. However, the collected data represented this way does not provide sufficient information for predictive design of inks with targeted rheology.

Predicting elasticity from particle interactions. To formulate a more predictive description, we look at how the elastic modulus G' of strongly flocculated dispersions is related to the particle interaction potential. For simplicity, we treat the colloids as individual particles of identical known diameters, without accounting for particle aggregates characteristic of fumed silica. If the total potential is approximated by the sum of the electrostatic and van der Waals contributions, the elastic modulus can be written as:[24]

$$G' \sim \frac{2\phi_{eff}^2}{D_0^2}\left(\frac{A_H}{12D_0} - C\zeta^2\right) \quad (3)$$

$$C = 2\pi\varepsilon\varepsilon_0 \ln[(1 - exp(-\kappa D_0))^{-1}] \quad (4)$$

where A_H is the Hamaker constant (6.42×10^{-20} J for SiO_2)[17], D_0 is the separation between particle surfaces, ζ is the zeta potential, ε is the dielectric constant, ε_0 is the permittivity of space, and κ^{-1} is the Debye screening length. For SiO_2-TBDA inks, knowing the TBDA volume fraction and assuming the entirety of the TBDA component is distributed evenly around each particle in a shell-like manner, D_0 can be approximated as the combined thickness of the TBDA coronae of two neighboring particles, d_{TBDA}:

$$d_{TBDA} = \sqrt[3]{\frac{3V_{shell}}{4\pi}} = \sqrt[3]{\frac{\phi_{TBDA}}{\phi_{SiO2}}\frac{a_{SiO2}^3}{8}} \quad (5)$$

The corresponding effective particle size and volume fraction account for both the particle and corona. (**Figure 4b**). The Debye screening length is calculated as:[24]

$$\kappa^{-1} = \sqrt{\frac{\varepsilon\varepsilon_0 kT}{\sum_i N_A e^2 z_i^2 c_i^2}} \quad (6)$$

where k is the Boltzmann constant, T is temperature, N_A is Avogadro's number, e is the proton charge, and z_i and c_i are the charge and concentration of species i, respectively.

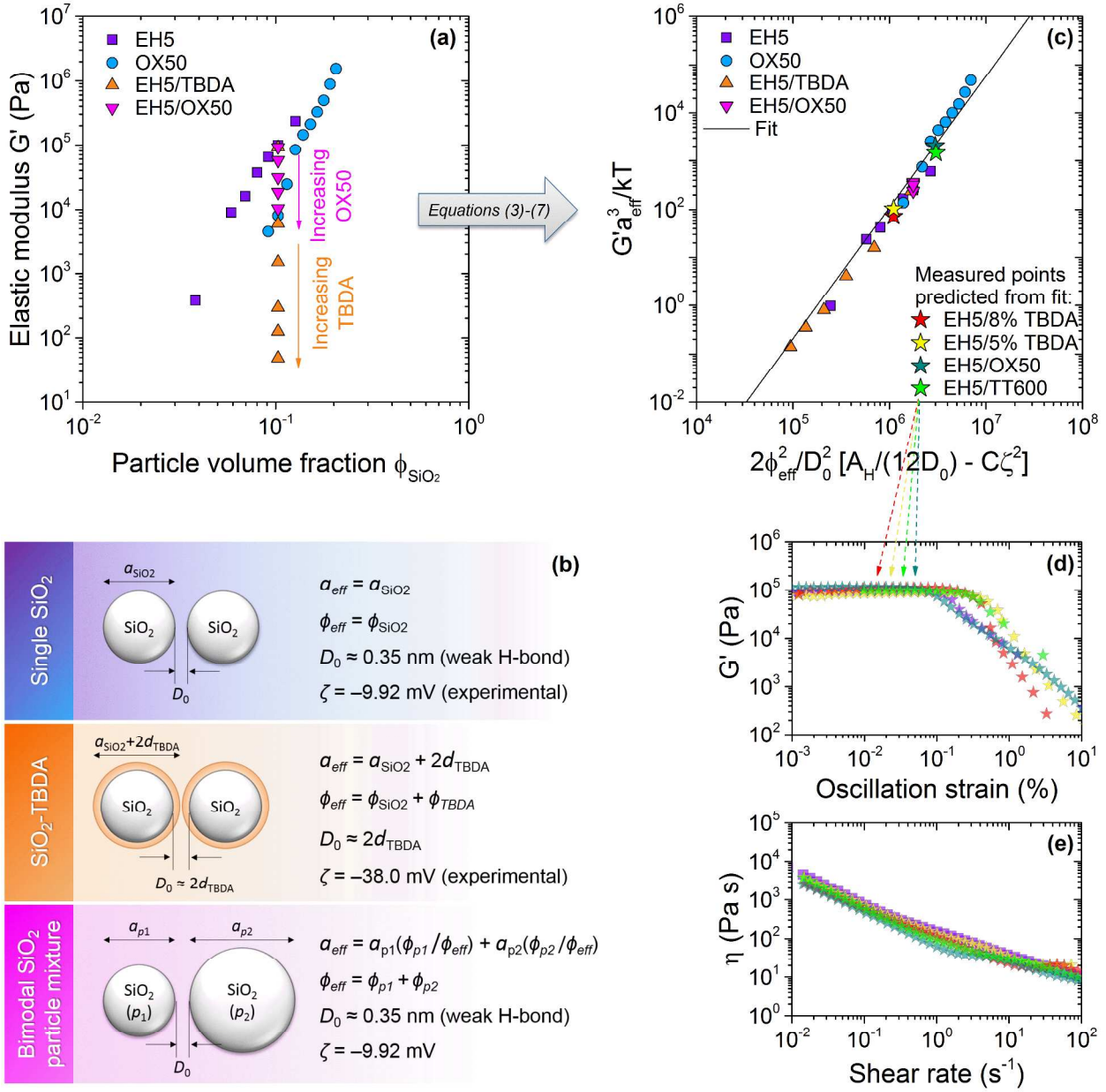

Figure 4. Effects of ink composition on the elastic modulus of the suspension. (a) Linear elastic modulus as a function of particle volume fraction collected from single particle type (EH5 and OX50), bimodal particle mixtures, and inks doped with TBDA. (Source data available in Figure S2.) **(b)** Schematic and parameter definitions used in the calculations. **(c)** All of the data collapses onto a single line when scaled using equations (3)-(7). The obtained model captures the effects of all the composition parameters and allows predictions of rheological behavior for arbitrary ink formulations from a single equation. **(d,e)** Different formulations of the same total solids loading predicted from the fit show viscoelastic properties well matched with the desired baseline ink behavior.

The zeta potential was experimentally measured for diluted silica (-9.92 mV) and silica-TBDA (-38.0 mV) inks in tetraglyme. Knowing that the attractions between silica particles in ether-like solvents are dominated by hydrogen bonding, as shown by Raghavan et al.,[17] the separation distance between particle surfaces D_0 for silica particles in tetraglyme was chosen as the length of a weak hydrogen bond (0.35 nm).

The elastic modulus can further be normalized by the particle size as:[23]

$$G^* = \frac{G' a_{eff}^3}{kT} \quad (7)$$

where a_{eff} is the effective particle size. For bimodal inks (two colloid sizes), a_{eff} is calculated as an average particle diameter based on the volume fractions of each particle (**Figure 4b**).

When the elastic modulus data is normalized using equations (3)-(7), all the data collapses onto a single line, described by $Y = 5\text{x}10^{-15} X^{2.72}$, where Y and X correspond to the expressions of the axes in **Figure 4c**. The data from inks doped with TBDA now aligns with the slope of SiO_2-only data, as interaction potentials decrease with increasing TBDA concentration due to a more negative zeta potential ζ and larger particle separation distances D_0. In addition, the data for bimodal mixtures of EH5 and OX50 particles tends to collapse onto a single point when scaled by the effective particle size a_{eff}. This indicates that we can capture the particle size distribution effect and use it to modify the particle ratios in formulations for a targeted elastic modulus. From the scaled fit, we are able to predict new formulations with matched total solids loadings (25.2 wt%, exact compositions given in Table S2) that all possess the desired rheological properties by aiming for a modulus of $G' = 10^5$ Pa. The inks formulated from predictions included TBDA-doped inks (at concentrations matching 5 wt% and 8 wt% TiO_2 in final glass), EH5/OX50 bimodal SiO_2 inks, as well binary mixtures of EH5 and a third fumed silica (AEROSIL® TT600). Even though the TT600 particle inks were not included in the original experimental data sets, we were able to predict their effects on mixture rheology based on the particle size. We find that the measured values of the properties of these predicted formulations (star symbols in **Figure 4c**) agree well with the rest of the data, and that the linear elastic moduli and viscosities of the formulations are in very good agreement (**Figures 4d and 4e**).

3D printing of silica-titania glass. The predicted ink formulations displayed good printability and were successfully processed into transparent glass. A multimaterial part was printed in a DIW setup by flowing two inks into a Y-shaped double-inlet, single-outlet 610 μm nozzle (**Figure 5a**). To produce a core-cladding structure (SiO_2-TBDA core, SiO_2-only cladding), the printing code was programmed to switch between the corresponding displacement pistons. Notably, the entire part was printed using the same extrusion parameters (print speed 10 mm/s, nozzle height 0.48 mm), with very similar flow and recovery behavior of each material during deposition. The printed part was subsequently heat treated to remove organics,[10] sintered to a glass at 1500 °C and polished by hand to a flat surface figure (**Figure 5b-d**). A video illustrating the imparted change in the refractive index of the produced glass can be found in the Supporting Information. The polished glass was then characterized for titania content across the diameter using an electron microprobe (**Figure 5e**). Due to a lag time associated with alternating between inks (not compensated for in the printing process), the switchover between the two materials is not instantaneous, which results in a more gradual change in composition. Improvements in extrusion control and capacitance compensation can be implemented for better regulation of material deposition. However, those efforts would exceed the scope of this manuscript and will instead be featured in a subsequent publication.

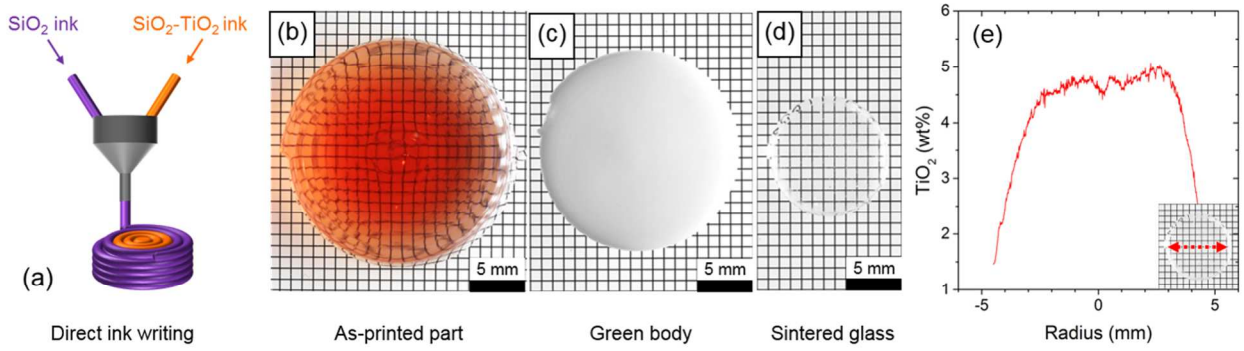

Figure 5. 3D printing and processing of a multimaterial glass. (a) Schematic of the direct ink write (DIW) nozzle (video of printing process available in Supporting Information). **(b)** 3D printed core-cladding structure (the TBDA-doped core was dyed with a few ppm of Sudan Red dye to visualize the composition difference). **(c)** SiO_2-TiO_2 green body after removal of all organic components. **(d)** Flat-polished SiO_2-TiO_2 glass sintered at 1500 °C. **(e)** TiO_2 concentration profile across the glass diameter as measured by electron microprobe. (See Supporting Information for video demonstrating the refractive index profile.)

▪ SUMMARY AND CONCLUSIONS

Control over the viscoelastic properties of materials for direct ink writing and other extrusion-based additive manufacturing processes is critical to the success of the fabrication technique. We have shown that the formulations of particle-based viscoelastic inks with matched solids loading and equivalent desired rheological properties can be predicted from interaction potential estimates and a small set of data under simple assumptions. Using this methodology, the elasticity and viscosity of a material can be predicted over a wide range of system parameters and tuned for the specific application. It should be noted that these predictions focus on the linear elasticity of the material, which describe the stiffness of the material at rest. The dynamic and transient characteristics of thixotropic materials during yielding and recovery are also very relevant,[25, 26] but fall beyond the scope of this study and will be focused on in a future publication. Nevertheless, this ability could greatly facilitate introducing new materials into an existing additive manufacturing production line without the necessity to re-evaluate the setup. Moreover, the approach provides a path to alleviate issues of mismatched ink properties in multimaterial printing. In addition, we have found that studying this system provided important insight into the nanoscale interactions taking place in suspensions of particles in organic solvents. While colloidal theories have typically been applied to particles in aqueous electrolyte environments, our results suggest that the particle interactions can be described in the same way for suspensions in organic solvents. We expect that this approach can be extended to other colloidal systems to predict flow behavior for a given set of extrusion parameters. For our system, the separation distance between particle surfaces was estimated as a length of a weak hydrogen bond; however, inter-particle distances in other systems could be determined by scattering or optical methods. Finally, we have demonstrated the 3D printing of multimaterial silica-titania glass with a spatial change in refractive index. This success presents a vital step towards the development of additively manufactured glass optics with tailored refractive index profiles.

▪ ACKNOWLEDGEMENTS

The authors gratefully acknowledge Micromeritics Analytical Services for performing zeta potential measurements and William Steele at Lawrence Livermore National Laboratory for glass polishing efforts. The AEROSIL® fumed silica powders were kindly provided to us by Evonik Industries at no cost. This work was performed under the auspices of the U.S. Department of Energy by Lawrence Livermore National Laboratory under Contract DE-AC52-07NA27344 within the LDRD program 16-SI-003. LLNL-JRNL-749401.

▪ SUPPORTING INFORMATION

Complete ink formulations, TEM images of fumed silica particles, and additional rheology data can be found in the Supporting Information.

▪ REFERENCES

(1) Lee, J.-Y.; An, J.; Chua, C. K. Fundamentals And Applications Of 3D Printing For Novel Materials. *Applied Materials Today* **2017,** *7*, 120-133.
(2) Schultz, P. C. Binary Titania-Silica Glasses Containing 10 To 20 Wt% Tio2. *Journal Of The American Ceramic Society* **1976,** *59*, 214-219.
(3) Jones, I. K.; Seeley, Z. M.; Cherepy, N. J.; Duoss, E. B.; Payne, S. A. Direct Ink Write Fabrication Of Transparent Ceramic Gain Media. *Optical Materials* **2018,** *75*, 19-25.
(4) Marchelli, G.; Prabhakar, R.; Storti, D.; Ganter, M. The Guide To Glass 3D Printing: Developments, Methods, Diagnostics And Results. *Rapid Prototyping Journal* **2011,** *17*, 187-194.
(5) Sing, S. L.; Yeong, W. Y.; Wiria, F. E.; Tay, B. Y.; Zhao, Z.; Zhao, L.; Tian, Z.; Yang, S. Direct Selective Laser Sintering And Melting Of Ceramics: A Review. *Rapid Prototyping Journal* **2017,** *23*, 611-623.
(6) Luo, J.; Pan, H.; Kinzel, E. C. Additive Manufacturing Of Glass. *Journal Of Manufacturing Science And Engineering* **2014,** *136*, 061024.
(7) Luo, J.; Gilbert, L. J.; Qu, C.; Landers, R. G.; Bristow, D. A.; Kinzel, E. C. Additive Manufacturing Of Transparent Soda-Lime Glass Using A Filament-Fed Process. *Journal Of Manufacturing Science And Engineering* **2017,** *139*, 061006.
(8) Luo, J.; Hostetler, J. M.; Bristow, D. A.; Landers, R. G.; Kinzel, E. C.; Goldstein, J. T. In *Heat Transfer In Additive Manufacturing Of Glass*, 2017; American Society Of Mechanical Engineers: PP V002T16A002-V002T16A002.
(9) Kotz, F.; Arnold, K.; Bauer, W.; Schild, D.; Keller, N.; Sachsenheimer, K.; Nargang, T. M.; Richter, C.; Helmer, D.; Rapp, B. E. Three-Dimensional Printing Of Transparent Fused Silica Glass. *Nature* **2017,** *544*, 337.
(10) Nguyen, D. T.; Meyers, C.; Yee, T. D.; Dudukovic, N. A.; Destino, J. F.; Zhu, C.; Duoss, E. B.; Baumann, T. F.; Suratwala, T.; Smay, J. E. 3D-Printed Transparent Glass. *Advanced Materials* **2017,** *29*, 1701181.
(11) Destino, J. F.; Dudukovic, N. A.; Johnson, M. A.; Nguyen, D. T.; Yee, T. D.; Egan, G. C.; Sawvel, A. M.; Steele, W. A.; Baumann, T. F.; Duoss, E. B. 3D Printed Optical Quality Silica And Silica–Titania Glasses From Sol–Gel Feedstocks. *Advanced Materials Technologies* **2018**, *3*, 1700323.
(12) Lewis, J. Direct Ink Writing Of 3D Functional Materials. *Advanced Functional Materials* **2006,** *16*, 2193-2204, Doi: 10.1002/Adfm.200600434.
(13) Li, W.; Ghazanfari, A.; Leu, M. C.; Landers, R. G. Extrusion-On-Demand Methods For High Solids Loading Ceramic Paste In Freeform Extrusion Fabrication. *Virtual And Physical Prototyping* **2017,** *12*, 193-205.

(14) Liravi, F.; Darleux, R.; Toyserkani, E. Additive Manufacturing Of 3D Structures With Non-Newtonian Highly Viscous Fluids: Finite Element Modeling And Experimental Validation. *Additive Manufacturing* **2017,** *13*, 113-123.
(15) Donovan, J. J.; Singer, J. W.; Armstrong, J. T. A New Epma Method For Fast Trace Element Analysis In Simple Matrices. *American Mineralogist* **2016,** *101*, 1839-1853.
(16) Armstrong, J. T. Citzaf-A Package Of Correction Programs For The Quantitative Electron Microbeam X-Ray-Analysis Of Thick Polished Materials, Thin-Films, And Particles. *Microbeam Analysis* **1995,** *4*, 177-200.
(17) Raghavan, S. R.; Walls, H. J.; Khan, S. A. Rheology Of Silica Dispersions In Organic Liquids: New Evidence For Solvation Forces Dictated By Hydrogen Bonding. *Langmuir* **2000,** *16*, 7920-7930.
(18) Weston, J. S.; Harwell, J. H.; Grady, B. P. Rheological Characterization Of Yield Stress Gels Formed Via Electrostatic Heteroaggregation Of Metal Oxide Nanoparticles. *Soft Matter* **2017,** *13*, 6743-6755.
(19) Breval, E.; Deng, Z.; Pantano, C. G. Microstructure Of Sol-Gel Processed TiO2/SiO2 Glasses. *Journal Of Non-Crystalline Solids* **1990,** *125*, 50-57.
(20) Deng, Z.; Breval, E.; Pantano, C. G. Colloidal Sol/Gel Processing Of Ultra-Low Expansion TiO2/SiO2 Glasses. *Journal Of Non-Crystalline Solids* **1988,** *100*, 364-370.
(21) Niederberger, M.; Cölfen, H. Oriented Attachment And Mesocrystals: Non-Classical Crystallization Mechanisms Based On Nanoparticle Assembly. *Physical Chemistry Chemical Physics* **2006,** *8*, 3271-3287.
(22) Zhang, H.; Banfield, J. F. Kinetics Of Crystallization And Crystal Growth Of Nanocrystalline Anatase In Nanometer-Sized Amorphous Titania. *Chemistry Of Materials* **2002,** *14*, 4145-4154.
(23) Mewis, J.; Wagner, N. J. *Colloidal Suspension Rheology*, Cambridge University Press: 2012.
(24) Larson, R. G. *The Structure And Rheology Of Complex Fluids*, Oxford University Press New York: 1999; Vol. 150.
(25) Zhu, C.; Smay, J. E. Thixotropic Rheology Of Concentrated Alumina Colloidal Gels For Solid Freeform Fabrication. *Journal Of Rheology* **2011,** *55*, 655-672.
(26) M'Barki, A.; Bocquet, L.; Stevenson, A. Linking Rheology And Printability For Dense And Strong Ceramics By Direct Ink Writing. *Scientific Reports* **2017,** *7*, 6017.

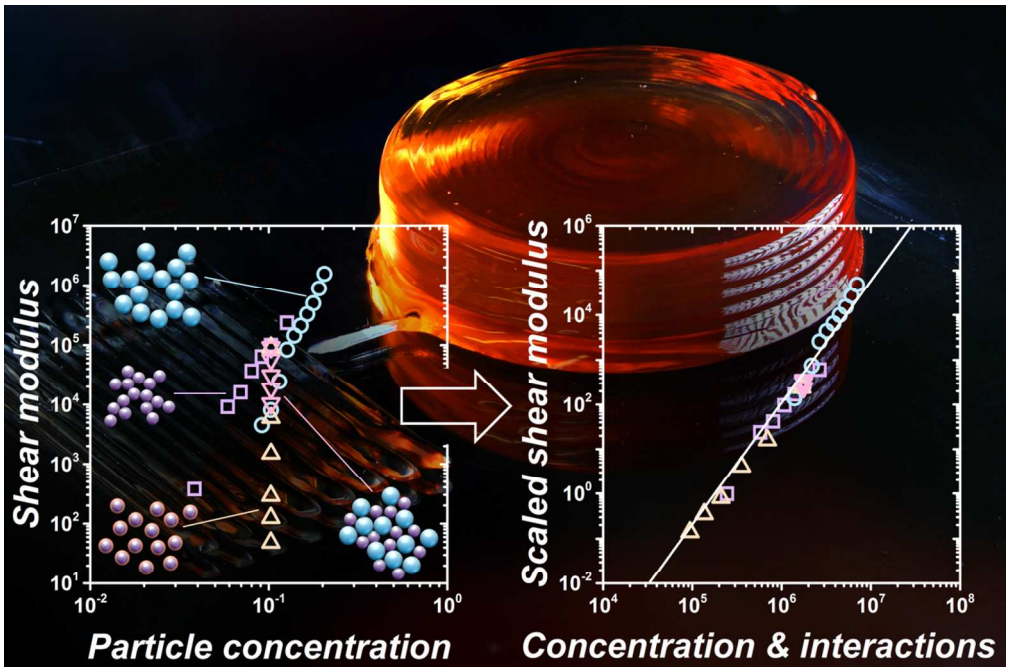

238x157mm (150 x 150 DPI)

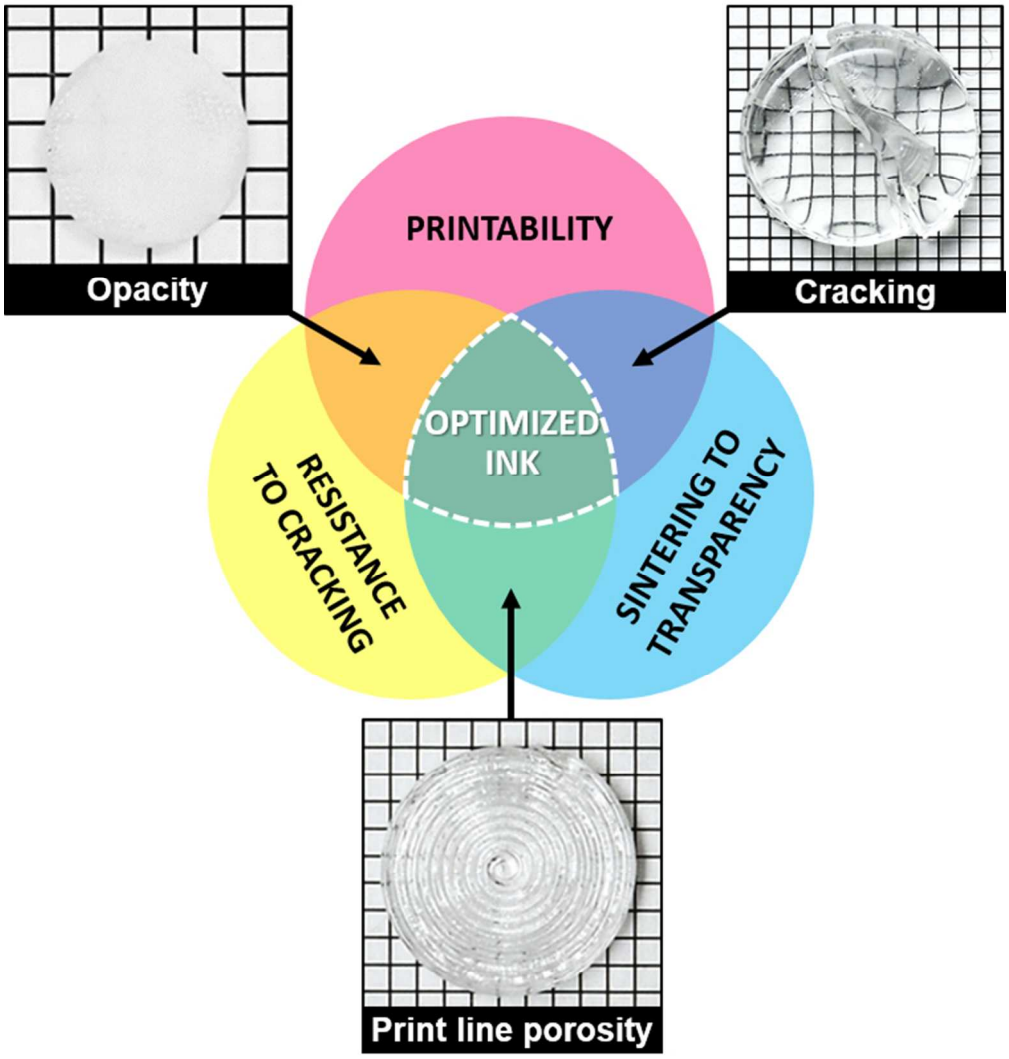

Figure 1. Ink formulation requirements. The post-print treatment is sensitive to chemical modification of the ink, which can result in unwanted subsequent porosity (i.e. lack of transparency) or decreased green body strength (i.e. cracking).

127x139mm (150 x 150 DPI)

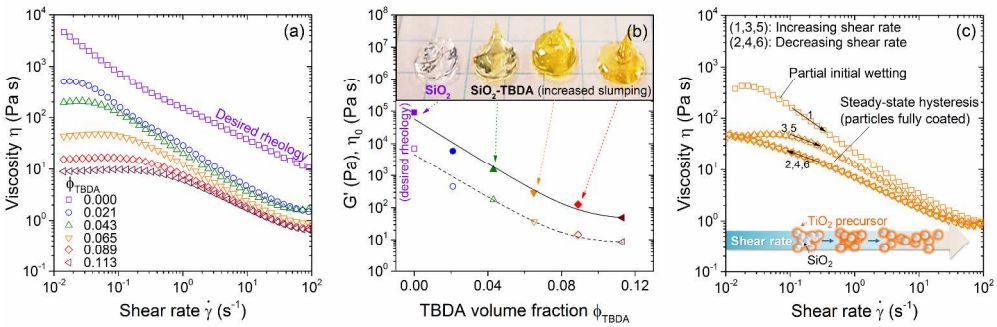

Figure 2. Effect of TiO_2 precursor (TBDA) concentration on ink rheology at constant SiO_2 volume fraction of φ = 0.103. (a) While the SiO_2-only ink is a yield stress fluid (gel) with no low-shear plateau, addition of TBDA changes the flow curve profile and exhibits a pronounced zero-shear viscosity, indicating the tendency of the TBDA inks to flow at rest. (b) The linear elastic modulus and low-shear viscosity show the same trend and decrease by three orders of magnitude over the TBDA range. (c) With increasing shear rate, flocs of silica particles are broken down and particles are uniformly coated with TBDA. Additional data available in Figures S2-S4.

635x208mm (300 x 300 DPI)

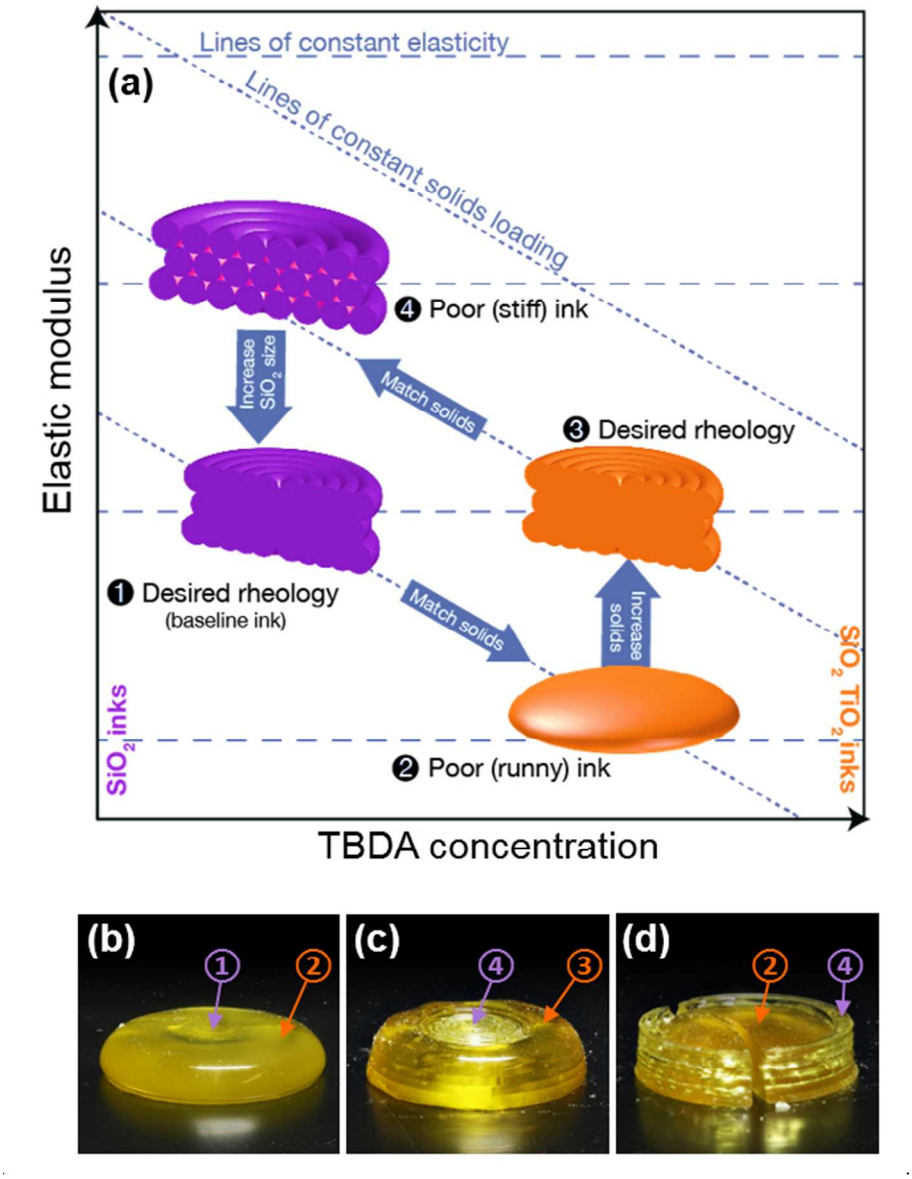

Figure 3. The need for simultaneous matching of the desired rheology and total solids concentration of two inks. (a) To avoid additional chemical species in the material, control over ink properties can instead be achieved by modifying the silica particle volume fraction and particle size/distribution. (b), (c) When printing two inks of the same solids concentration but disparate rheological properties, the inks exhibit different printability. (d) When inks are mismatched in both rheology and solids concentration, in addition to incompatible printability, cracking due to differential shrinkage stresses occurs even during room temperature air drying.

115x153mm (150 x 150 DPI)

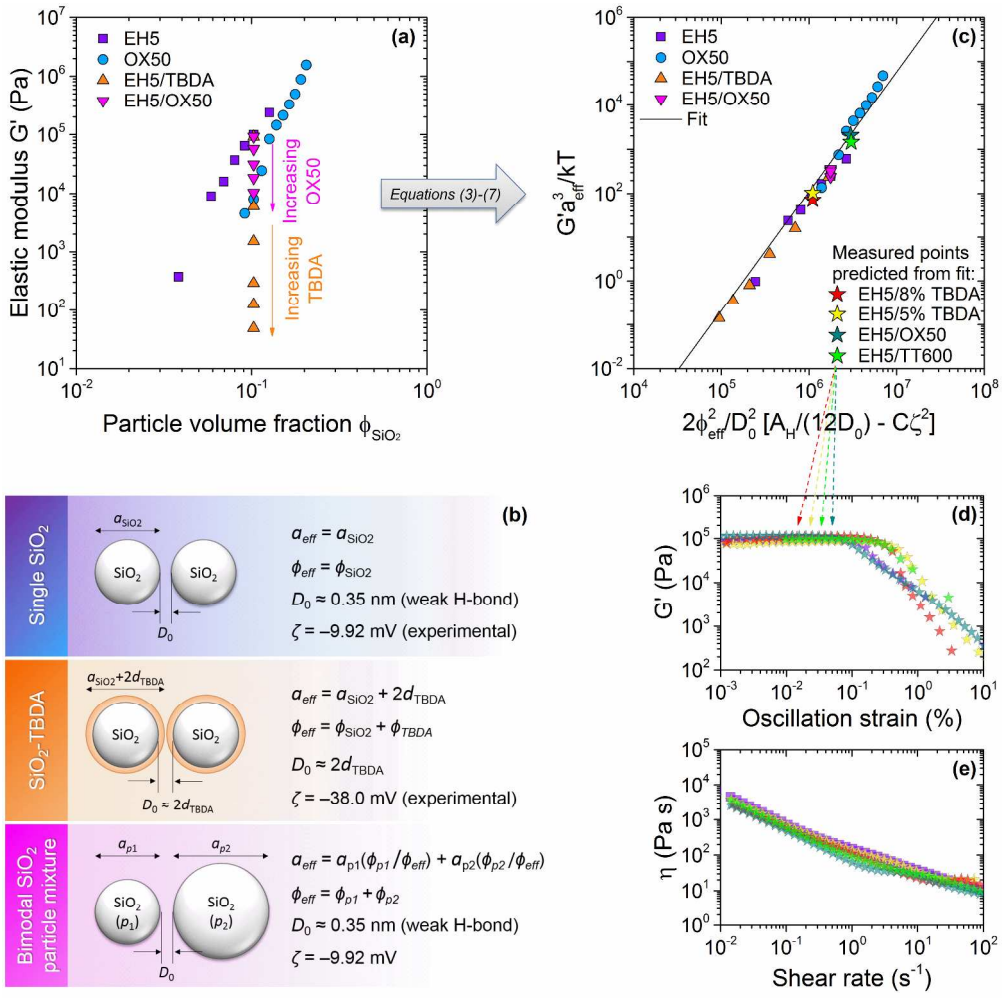

Figure 4. Effects of ink composition on the elastic modulus of the suspension. (a) Linear elastic modulus as a function of particle volume fraction collected from single particle type (EH5 and OX50), bimodal particle mixtures, and inks doped with TBDA. (Source data available in Figure S2.) (b) Schematic and parameter definitions used in the calculations. (c) All of the data collapses onto a single line when scaled using equations (3)-(7). The obtained model captures the effects of all the composition parameters and allows predictions of rheological behavior for arbitrary ink formulations from a single equation. (d,e) Different formulations of the same total solids loading predicted from the fit show viscoelastic properties well matched with the desired baseline ink behavior.

457x457mm (300 x 300 DPI)

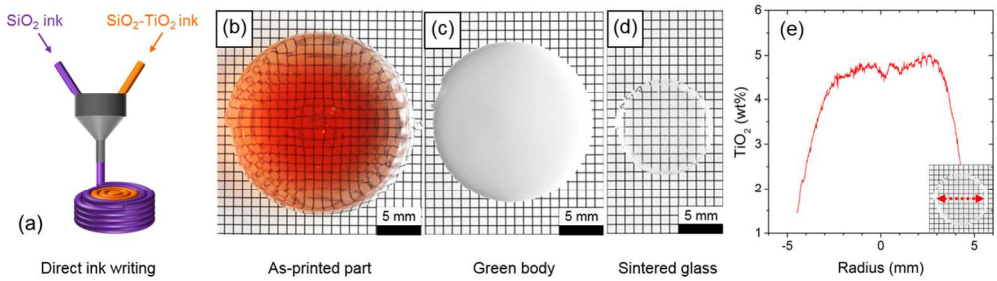

Figure 5. 3D printing and processing of a multimaterial glass. (a) Schematic of the direct ink write (DIW) setup (video of printing process available in Supporting Information). (b) 3D printed core-cladding structure (the titania-doped core was dyed with a few ppm of Sudan Red dye to visualize the composition difference). (c) SiO_2-TiO_2 green body after removal of all organic components. (d) Flat-polished SiO_2-TiO_2 glass sintered at 1500 °C. (e) TiO_2 concentration profile across the glass diameter as measured by electron microprobe. (See Supporting Information for video demonstrating the refractive index profile.)

236x68mm (150 x 150 DPI)